J. MATER. CHEM., 1994, 4(5), 689–694

Vapour-phase Synthesis of Titanium Nitride Powder

Jan Pieter Dekker,*[a,b] Paul J. van der Put,[a] Hubert J. Veringa[b] and Joop Schoonman[a]
[a] *Laboratory for Applied Inorganic Chemistry, Delft University of Technology, Julianalaan 136, 2628 BL Delft, The Netherlands*
[b] *ECN, Energy Research Foundation, Westerduinweg 3, 1755 ZG Petten, The Netherlands*

Titanium nitride powder has been synthesized using titanium tetrachloride, ammonia and hydrogen. The influence of the reaction temperature on stoichiometry, particle size and production rate in the gas phase has been investigated. Crystalline titanium nitride powders were formed in all cases. The observed lattice parameter of the powders as a function of reaction temperature suggests that only at high reaction temperatures can a stoichiometric titanium nitride powder be formed. In the temperature range 900–1173 K the mean primary particle size varies between 100 and 200 nm, and the geometric standard deviation varies between 1.1 and 1.3 for the powders formed below a reaction temperature of 1173 K. A significantly smaller primary particle size is observed at higher reaction temperatures. A fractal dimension analysis indicates that at low reaction temperatures the powders are not agglomerated.

There is a demand for sintered ceramic products with increased hardness and strength. Submicrometre powders are desired to fabricate such products, because these yield a fine microstructure with uniform chemical composition. Non-oxide powders are attractive for the production of sintered parts because of their high melting points, high-temperature strengths, high hardness and corrosion resistance. Because of these requirements titanium nitride (TiN) is an attractive material. For example, it might be a substitute for tungsten carbide in cutting tools and wear-resistant parts.[1] In addition, the vapour-phase synthesis of TiN powder is an important prerequisite of the particle precipitation aided chemical vapour deposition process of TiN. Non-oxide powders can be produced by gas-phase reactions,[2] solid-state reactions,[3,4] or thermal decomposition of solids.[5] Gas-phase reactions at high temperatures, such as the oxidation of metal halides have been proven to be a cost-effective method to produce uniform submicrometre particles with high purity.[6] The kinetics of formation of these oxide particles such as titania (TiO_2) and silica (SiO_2) have been investigated extensively.[7–9] The formation of several metal nitrides in the gas phase at high temperatures using their respective metal halides and ammonia (NH_3) has been shown to be possible as well.[2,10,11] Although the criteria for the synthesis of these solids in the gas phase are not well understood, the formation of a solid in the gas phase seems to be dependent on the thermodynamic equilibrium constant. In general, a homogeneous reaction will only occur if the equilibrium constant of the reaction is sufficiently high.[2] TiN can be formed at high temperatures using titanium tetrachloride ($TiCl_4$), hydrogen (H_2) and NH_3, according to the overall reaction,

$$2TiCl_4(g)+2NH_3(g)+H_2(g)\rightarrow 2TiN(s)+8HCl(g) \quad (1)$$

We believe that the production of TiN powders can be a cost-effective method, because this chemical route involves rather cheap chemicals. However, reports on the formation of this metal nitride are scarce.[2,11,12] Kato's group[2,10,11] have investigated among other metal nitrides and metal carbides the TiN formation in the gas phase. The reduction of $TiCl_4$ with magnesium (Mg) in a nitrogen atmosphere has been reported to be effective for the production of TiN.[1] However, a disadvantage is that Mg itself is an impurity source.

We have investigated the synthesis of TiN powder using $TiCl_4$, NH_3, and H_2 at a high temperature. The influence of the reaction temperature on stoichiometry, particle size, and production rate in the gas phase has been investigated. The stoichiometry is determined by XRD analysis, and particle sizes are obtained by quasi-elastic light scattering (QELS) analysis,[13] sedimentation field flow fractionation (SdFFF) analysis,[14,15] and SEM/TEM analysis. The diffusion coefficient of small particles in dilute liquid suspensions can be measured with QELS analysis or the photon correlation spectroscopy technique. Here, the autocorrelation function of the intensity of laser light, scattered by particles in a dilute liquid suspension is calculated. This power spectrum of scattered light allows determination of the particle diffusion coefficient, which can easily be correlated to a particle diameter if it is assumed that the particles are spherical and have a relatively monodisperse particle size distribution. A powder suspended in water can be fractionated by the SdFFF technique. In SdFFF a suspension flows through a force field in a centrifuge. The mass distribution of the dispersed powder is exponentionally distributed in the field as a result of the counteracting combination of Brownian diffusion and centrifugal force. Owing to this induced mass distribution within the laminar flow, the retention time of particles in the apparatus is a function of their weight. The retention time of the particles can be correlated to their mass. This technique can be used to fractionate the powder to obtain dilute particle suspensions with narrow size distributions for QELS analysis.

Often, gas-phase synthesis results in the formation of agglomerates. For many applications this is undesirable. The determination of the fractal dimension of the powder from TEM micrographs can provide information on the history of the agglomerates.[16,17] The fractal dimension of an agglomerate describes the relation between the mass (M) or the number of particles (N) and the radius (R) containing them:

$$M \propto R^{D_f}$$

or

$$N \propto R^{D_f} \quad (2)$$

The second relation is only valid for clusters consisting of monosized particles. The fractal dimension (D_f) depends on certain features of the agglomerate-formation processes. For example, if the cluster is formed in two-dimensional space according to a particle–cluster diffusion-limited aggregation process, then the fractal dimension is expected to be *ca.* 1.7, while a cluster–cluster diffusion-limited aggregation will yield a fractal dimension of <1.5.[18–20] Ballistic aggregation processes will often yield higher fractal dimensions, *e.g.* a particle–cluster ballistic aggregation will lead to a dimension of more than 1.9, and a cluster–cluster ballistic aggregation will give a dimension of more than 1.5.[18–20]

Experimental

A cylindrical reactor (inner diameter = 50 mm, length = 700 mm) with, on the inside, a TiN coating in a three-zone furnace equipped with resistive heating was used for the synthesis experiments. In this set-up, the $TiCl_4$ is fed into the reactor by a hydrogen carrier gas. This hydrogen is bubbled through heated $TiCl_4$ in order to saturate the hydrogen stream with reactant vapour. The $TiCl_4$ concentration in the H_2 stream is calculated assuming the $TiCl_4$ vapour pressure to be in equilibrium with the $TiCl_4$ liquid. A nozzle is used for the separated introduction of the reactants. H_2 and NH_3 flow through the inner side of this nozzle, whereas $TiCl_4$, H_2 and N_2 are introduced at the entrance of the reactor outside the nozzle. Thus, the reactants for homogeneous reaction are mixed at a high temperature, *i.e.* at the beginning of the second heating zone of the furnace. An excess of H_2 is used for the reduction of the titanium-containing vapour species to minimize incorporation of chlorine in the powder.

In the third heating zone of the reactor a cold finger is placed to collect a representative amount of the powder for further analysis. The cold finger is cooled from the inside by pressurized air. For the experiments as a function of reaction temperature an NH_3 excess of 10 with respect to $TiCl_4$ is used. The reaction temperature of the second heating zone of the reactor is varied from 900 to 1300 K, and the gas-phase temperature in the third heating zone of the furnace is kept constant at 865 K. For most experiments the temperature of the tip of the cold finger is kept constant at 800 K. The experimental conditions are summarized in Table 1.

The TiN powder collected on the cold finger in the third heating zone of the furnace is suspended in an aqueous ammonia solution (0.002 mol dm^{-3}) with a powder concentration of typically 1–2 wt.%. This suspension is fractionated by a Dupont SF[3] analyser. The same instrument conditions were used as reported by Scarlett *et al.*,[15] and the Dupont SF[3] computer program was used for the particle-size distribution calculations. The fractionated suspensions are collected in optical cuvets, and these suspensions are analysed by a Coulter N4 light scattering analyser. TEM grids and polished silicon pieces are dipped in ethanol suspensions with a powder concentration of a few weight percent for TEM and SEM analysis, respectively. Screen printings of the TEM micrographs are used for the determination of the fractal dimension. The negative of the screen used yields white pixels on the TEM micrographs where particles are present. Each white pixel represents a certain amount of mass visualized by the screen on the TEM micrograph. The number of white pixels is counted as a function of the radius for each agglomerate. The fractal dimension can be obtained by fitting the data according to eqn. (2).

Table 1 Process parameters for the synthesis of TiN powder

inside nozzle	NH_3 flow	0–140 μmol s^{-1}
	H_2 flow	0.39–0.20, 0.78 mmol s^{-1}
	total flow	0.39, 0.78 mmol s^{-1}
outside nozzle:	$TiCl_4$ flow	7–24, 35 μmol s^{-1}
	N_2 flow	0, 0.49 mmol s^{-1}
	H_2 flow	0.38–0.49 mmol s^{-1}
	total flow	0.54, 1.015 mmol s^{-1}
reaction time		1800, 3600 s
reaction temperature (second heating zone)		900–1300 K
gas phase temperature (third heating zone)		865 K
tip of cold finger		800–865 K
reactor pressure		1×10^5 Pa

Results and Discussion

The dark-brown titanium nitride powders formed were crystalline in all cases. Three characteristic XRD diffractograms are presented in Fig. 1. These results are in agreement with the reports of Hojo and Kato,[11] who observed that $TiCl_4$ and NH_3 react in the gas phase above 800 K to form a crystalline TiN powder. The lattice parameter of the powders as a function of reaction temperature is presented in Fig. 2.[21,22] There is an increase in lattice parameter with increasing reaction temperature. If it is assumed that the impurities in the powder are negligible, and that the composition of the powder varies only with respect to the stoichiometry then the lattice parameter can be correlated to the amount of nitrogen present in the TiN lattice. The lattice parameter of TiN_y as a function of the stoichiometry number y is presented in Fig. 3. A comparison of Fig. 2 and 3 suggests that only at high

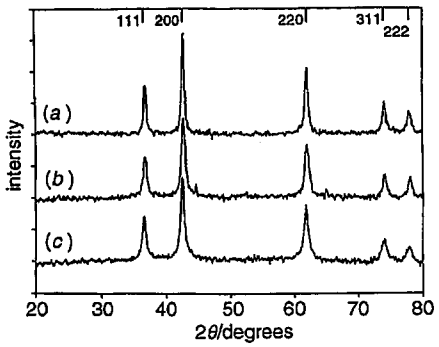

Fig. 1 XRD patterns of TiN powder synthesized at three different temperatures: (*a*) 923 K, (*b*) 973 K and (*c*) 1023 K

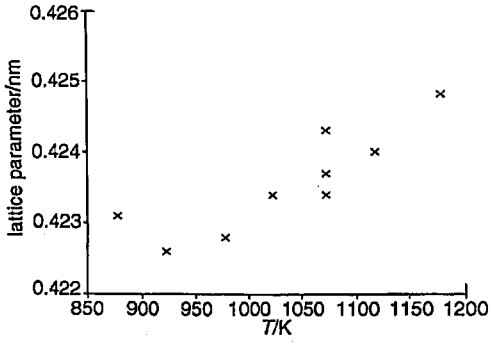

Fig. 2 Lattice parameter of fcc TiN powder as a function of reaction temperature

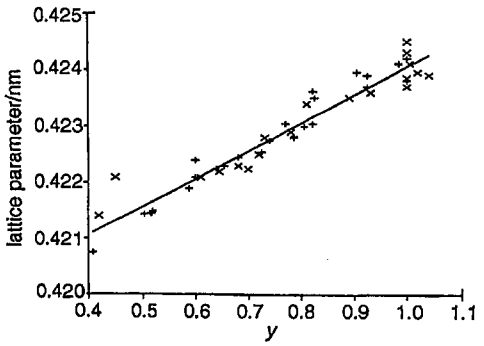

Fig. 3 Lattice parameter of fcc TiN_y as a function of nitrogen content y. Data from ref. 21 (×) and 22 (+)

reaction temperatures can stoichiometric titanium nitride powder be formed.

Particle sizes are obtained from SEM, TEM, QELS and SdFFF analyses. The particle size appears to be unaffected by the reactant concentrations. Only at lower $TiCl_4$ and NH_3 concentrations do the particle sizes tend to be smaller. In the temperature range 900–1173 K the mean primary particle size varies between 100 and 200 nm, as identified by TEM analysis. Particle-size distributions, typical for the experiments using a reaction temperature lower than 1173 K, are shown on the SEM and TEM micrographs in Fig. 4 and 5, respectively. A significantly smaller primary particle size is observed at higher reaction temperatures as can be seen in Fig. 6. All these

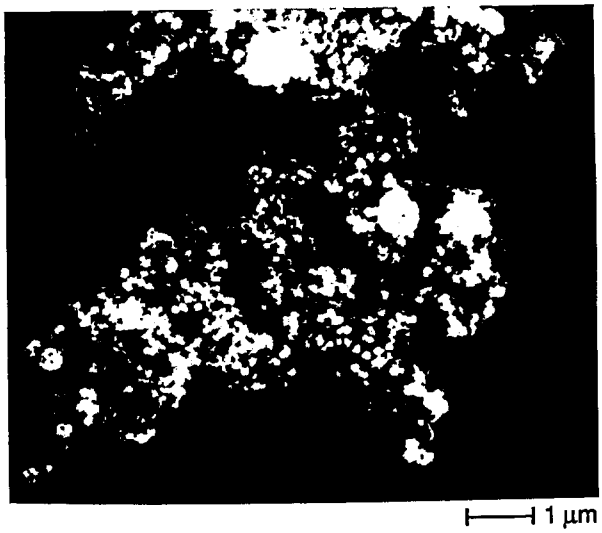

Fig. 4 SEM micrograph of TiN powder, typical for synthesis experiments within the temperature range 923–1173 K

Fig. 5 TEM micrograph of TiN powder, typical for synthesis experiments within the temperature range 923–1173 K

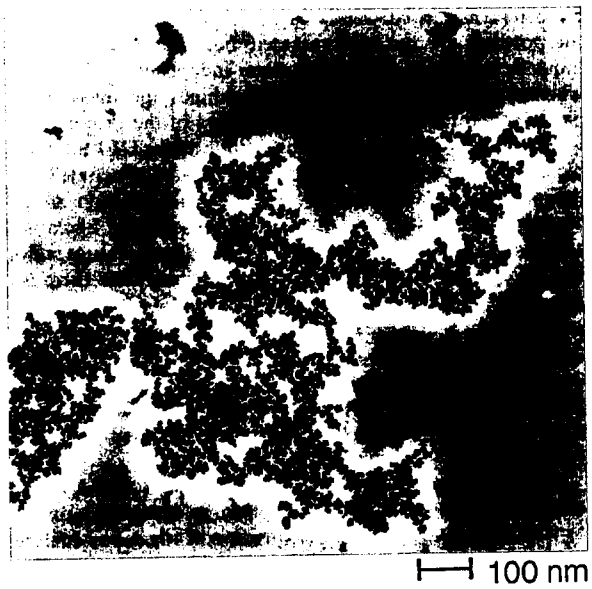

Fig. 6 TEM micrograph of TiN powder using a reaction temperature of 1223 K

particle sizes tend to be larger than the mean particle sizes reported by Kato *et al.*[2] as can be seen in Table 2.

The mass mean diameters derived from SdFFF analysis of suspended powders are typically between 200 and 300 nm, and the geometric standard deviation $\sigma_{(84.13/50)}$ varies between 1.1 and 1.3 for the powders formed below a reaction temperature of 1173 K. These diameters are in reasonable agreement with the diameters obtained from the QELS analysis, where the fractionated suspension corresponds to the mean mass diameter of the SdFFF analysis, as can be seen in Fig. 7. There is good agreement between the QELS diameters using all the fractionated samples and their corresponding SdFFF

Table 2 Specific surfaces and mean particle diameters derived from BET measurements and TEM micrographs

	Kato *et al.*		this paper	
T/K	d_{TEM}/nm	S_{BET}/m^2 g^{-1}	d_{TEM}/nm	S_{BET}/m^2 g^{-1}
973	110	16	172	33
1073			133	7–32
1173	70	19	185	17
1273			16	
1373	50			

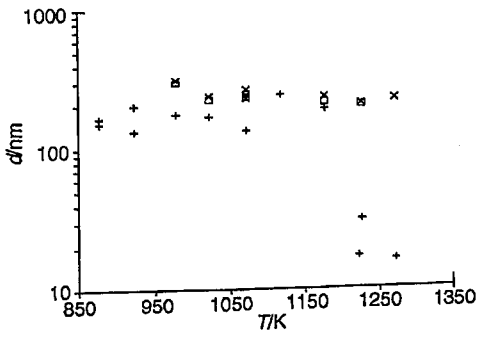

Fig. 7 Mean particle diameter as a function of reaction temperature using different particle size analysis techniques: ×, SdFFF; □, QELS; +, TEM

diameters, as can be seen in Fig. 8. This is an indication that the powders are not agglomerated, because the QELS technique determines a particle diameter independent of its mass, whereas the SdFFF technique determines the mass of the particles. Moreover, the TEM diameters of the primary particles are of the same order of magnitude as the QELS/SdFFF diameters. Thus, from these results it can be concluded that the primary particle size is only a weak function of the reaction temperature, and that it is not likely that agglomerates in the gas phase are formed within the temperature region from 923 to 1173 K. At high reaction temperatures there is a considerable mismatch between the TEM particle diameters and the QELS/SdFFF diameters. This is an indication that the particles are agglomerated. Apparently, a high reaction temperature results in the formation of agglomerated particles. The conclusion that the particles become agglomerated during the synthesis process can be confirmed by a fractal-dimension analysis of the TEM micrographs.

In all cases, agglomerates are found on the TEM micrographs. The degree of agglomeration is dependent on the powder concentration of the suspension. Thus, these agglomerates have to be a result of the preparation method for TEM samples. Agglomeration in the liquid film on the TEM grid occurs during evaporation of the medium. This agglomeration process is a typical two-dimensional diffusion-limited process. In principle, two different agglomeration processes are likely to occur on the TEM grid, *i.e.* a particle–cluster aggregation or a cluster–cluster aggregation. If a fractal dimension is found which is characteristic for a particle–cluster aggregation then it is likely that all the agglomerates are formed on the TEM grid, and not in the gas phase during the synthesis process. It is very unlikely that particle–cluster agglomerates can be formed in the gas phase, because each cluster present in the gas phase will agglomerate with other clusters as well. The fractal dimension for different agglomerates formed at two reaction temperatures is determined according to the circle method on TEM micrographs.[18] TEM micrographs of agglomerates were taken which were thought to be representive for all the inspected agglomerates on the TEM grid. The experimental fractal dimensions along with the expected values based on computer simulations are given in Table 3.

An example of a computer-simulated particle–cluster diffusion-limited aggregate ($D_f=1.7$) is presented in Fig. 9. The choice of centre for the fractal dimension determination of a computer-simulated agglomerate by the circle method is straightforward. However, the determination of such a centre of an agglomerate on a TEM micrograph is far more difficult. We have chosen for the middle of the agglomerates $\frac{1}{2}W$, and $\frac{1}{2}L$ as a centre for the circle method. In Table 3 the number of particles is equal to the total number of particles within the largest radius used for the fractal-dimension determination.

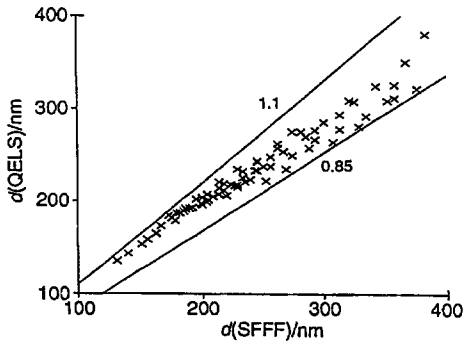

Fig. 8 QELS diameter using the fractionated suspensions from the SdFFF analysis as a function of the corresponding SdFFF diameter

Table 3 Mass fractal dimension for TiN agglomerates synthesized at two different temperatures

T/K	number of particles	L/W[a]	calculated 2D dimension	expected 2D dimension
1073	1591	1.3	1.69±0.09	1.71 (P-C)[b]
1073	77	1.4	1.80±0.14	1.71 (P-C)
1073	193	1.75	1.68±0.08	1.71 (P-C)
1073	447	1.42	1.75±0.06	1.71 (P-C)
1223	342	1.5	1.33±0.04	1.44 (C-C)[c]
1223	312	1.67	1.18±0.07	1.44 (C-C)
1223	742	1.71	1.41±0.02	1.44 (C-C)

[a]Agglomerate length over width ratio; [b]Particle-cluster diffusion limited aggregation;[18–20] [c]Cluster-cluster diffusion limited aggregation.[18–20]

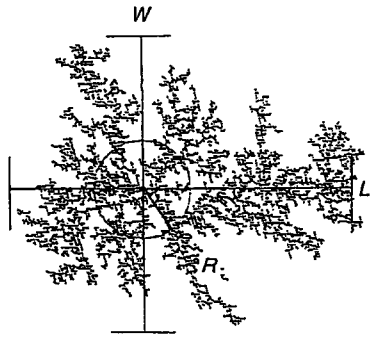

Fig. 9 Computer-simulated diffusion-limited particle–cluster aggregation. The meaning of L, W, and R is illustrated.

For agglomerates formed at a reaction temperature of 1073 K a fractal dimension is observed which is typical for a particle–cluster agglomeration. As mentioned before, it is very unlikely that such an process can occur during gas-phase synthesis. Hence, it can be assumed that this powder is not agglomerated. The observed fractal dimensions at a reaction temperature of 1223 K suggest that the particles collected in the reactor are already agglomerated. This is in agreement with the TEM and QELS/SdFFF analyses. It should be noted that a three-dimensional cluster–cluster diffusional aggregation will result in a fractal dimension of 1.78.[18–20] This value is close to the experimental fractal dimensions for powders formed at a reaction temperature of 1073 K. However, TEM images of the samples in a tilted position reveal that the agglomerates on the TEM grid are virtually two-dimensional.

The driving force for powder collection on the cold finger in the reactor is thermophoresis. The thermophoretic velocity (v_t) is proportional to the temperature gradient.[23]

$$v_t = -K\left(\frac{\nu}{T}\right)\nabla(T) \qquad (3)$$

where K is a constant for a given particle size, ν the kinematic viscosity of the gas, and T the temperature. In this case, where particles have a Knudsen number of order unity, K is only a weak function of the particle diameter.[24] Indeed, an increase in the amount of deposited material is observed with increasing temperature gradient. However, a quantitative analysis of the collection efficiency is not possible, because the gas-phase temperature near the cold finger has a complex non-linear dependence with respect to the axial and radial position. However, if the temperature of the cold finger and the temperature of the gas phase are kept constant then the weight of the harvested powder, which is a measure of the total TiN mass concentration in the gas phase, can be used to study the kinetics of the gas-to-particle conversion in the

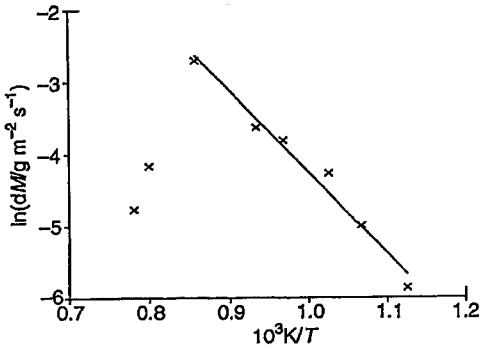

Fig. 10 Arrhenius plot of collected TiN powder mass rate on cold finger

reactor. The powder weight collection rate as a function of the reaction temperature is presented in an Arrhenius plot in Fig. 10. The maximum experimental collection efficiency is 5% given these experimental conditions. The gas-to-particle conversion shows an Arrhenius-like behaviour within the temperature range 923–1173 K. The apparent activation energy of the powder-formation process in this reactor is 94 kJ mol^{-1}. This apparent activation energy is determined by a combination of nuclei formation, particle growth and loss of reactant to the reactor walls. The contribution of the particle growth to the observed apparent activation energy can be eliminated by dividing the amount of harvested material by the particle mass with a mean primary particle diameter as derived from TEM analysis. This yields an apparent activation energy of 142 kJ mol^{-1} for the entire temperature region as can be seen in Fig. 11. This activation energy is related to the formation process of nuclei in the reactor. The observed decrease in particle growth can be ascribed to an increase in loss of reactant to the reactor wall or a change in growth mechanism. For example, a change in growth mechanism might be conceivable, if the reaction rate involving $TiCl_3$ as reactant is smaller than the reaction rate involving $TiCl_4$. Because, thermodynamic equilibrium calculations reveal that in the temperature region where the decrease in powder formation is observed the homogeneous equilibrium concentration of $TiCl_4$ decreases, and $TiCl_3$ becomes the most abundant titanium gas-phase species.[12] However, given the present experimental configuration, it can not be concluded what is the precise reason for the observed decrease in growth rate of the particles. Apparently, at low reaction temperatures the particle size characteristics are determined by a heterogeneous growth on the nucleus, whereas at high reaction temperatures the particle size characteristics are determined by the nucleus formation process itself.

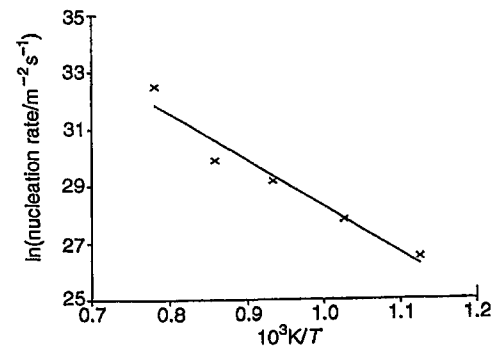

Fig. 11 Arrhenius plot of collected mass on cold finger divided by the particle mass with the mean primary particle diameter, *i.e.* proportional the nucleation rate in the reactor

Conclusions

Crystalline titanium nitride powders using $TiCl_4$, NH_3, and H_2 were formed in all cases. The lattice parameter of the powders as a function of reaction temperature suggests that only at high reaction temperatures can a stoichiometric titanium nitride powder be formed. In the temperature range 900–1173 K the mean primary TEM particle size varies between 100 and 200 nm. The mass mean diameters derived from SdFFF analysis of suspended powders are typically between 200 and 300 nm, and the geometric standard deviation varies between 1.1 and 1.3 for the powders formed below a reaction temperature of 1173 K, and a comparison between the results of the QELS and the SdFFF techniques indicates that the powders are not agglomerated. At high reaction temperatures there is a considerable mismatch between the TEM particle diameters and the QELS/SdFFF diameters. This is an indication that these particles are agglomerated. This phenomenon is confirmed by a fractal dimension analysis of the TEM micrographs. The gas-to-particle conversion shows an Arrhenius-like behaviour within the temperature region 923–1173 K. The apparent activation energy of the powder formation process in this reactor is 94 kJ mol^{-1}. From this result and the measured mass increase an activation energy of 142 kJ mol^{-1} for the homogeneous gas-phase reaction can be derived.

Glossary

d_{TEM}	mean primary particle diameter derived from TEM micrograph (nm)
D_f	fractal dimension
L	length of an agglomerate on a TEM micrograph
K	thermophoretic velocity constant
M	mass of a part of an agglomerate within radius R
N	number of particles of an agglomerate within radius R
R	radius
S_{BET}	specific surface area derived from BET analysis (m^2 g^{-1})
T	temperature (K)
v_t	thermophoretic velocity (m s^{-1})
W	width of an agglomerate on a TEM micrograph
y	stoichiometric number of TiN_y
$\sigma_{(84.13/50)}$	geometric standard deviation
ν	kinematic gas viscosity (m^2 s^{-1})

References

1 G. W. Elger, D. E. Traut, G. J. Slavens and S. J. Gerdemann, *Metall. Trans. B*, 1989, **20**, 493.
2 A. Kato, J. Hojo and Y. Okabe, *Mem. Fac. Eng. Kyushu Univ.*, 1981, **41**, 319.
3 M. Yoshimura, M. Nishioka and S. Sōmiya, *J. Mater. Sci. Lett.*, 1987, **6**, 1463.
4 H. Kudo and O. Odawara, *J. Mater. Sci.*, 1989, **24**, 4030.
5 E. Rothman, J. Stitt and H. K. Bowen, *Ceram. Industry*, 1985, 24.
6 S. E. Pratsinis and S. V. R. Mastrangelo, *Chem. Eng. Progr.*, 1989, **85**, 62.
7 S. E. Pratsinis, H. Bai, P. Biswas, M. Frenklach and S. V. R. Mastrangelo, *J. Am. Ceram. Soc.*, 1990, **73**, 2158.
8 M. K. Akhtar, S. E. Pratsinis and S. V. R. Mastrangelo, *J. Am. Ceram. Soc.*, 1992, **75**, 3408.
9 W. G. French, L. J. Pace and V. A. Foertmeyer, *J. Phys. Chem.*, 1978, **82**, 2191.
10 Y. Okabe, J. Hojo and A. Kato, *Yogyo Kyokai*, 1977, **85**, 173.
11 J. Hojo and A. Kato, *Yogyo Kyokai*, 1981, **89**, 277.

12 J. P. Dekker, P. J. van der Put, H. J. Veringa and J. Schoonman, in *Proc. Eighth Conf. Chemical Vapour Deposition*, ed. M. L. Hitchman and N. J. Archer, *J. Physique IV*, 1991, p. C2–592.
13 *Measurement of Suspended Particles by Quasi Elastic Light Scattering*, ed. B. E. Dahneke Wiley, 1983.
14 J. C. Giddings, S. K. Ratamathanawongs and H. M. Moon, *Kona*, 1991, **9**, 200.
15 B. Scarlett, H. G. Merkus, Y. Mori and J. Schoonman, *Particle Size Analysis*, ed., P. J. Lloyd, Wiley, 1992, p. 107.
16 J. L. LaRosa and J. D. Cawley, *J. Am. Ceram. Soc.*, 1992, **75**, 1981.
17 R. J. Samson, G. W. Mulholland and J. W. Gentry, *Langmuir*, 1987, 272.
18 R. Julien and R. Botet, *Aggregation and Fractal Aggregates*, World Scientific Publishing, Singapore, 1986.
19 *The Fractal Approach to Heterogeneous Chemistry*, ed. D. Avnir, Wiley, Chichester, 1989.
20 *Trends in Aerosol Research*, ed. A. Schmidt-Ott, Universität Duisburg, 1990.
21 H. J. M. Rypkema, MSc Thesis, Delft University of Technology, 1986.
22 W. Wakelkamp, PhD Thesis, Eindhoven University of Technology, 1991.
23 P. G. Simpkins, S. Greenberg-Kosinski and J. B. MacChesney, *J. Appl. Phys.*, 1979, **50**, 5676.
24 L. Talbot, R. K. Cheng, R. W. Schefer and D. R. Willis, *J. Fluid. Mech.*, 1980, **101**, 737.

Paper 3/06945A; *Received* 22*nd November*, 1993